Article

Discovery Medicine 2025; 37(200): 2055–2064
https://doi.org/10.24976/Discov.Med.202537200.176

Th2-Mediated IL-4/PI3K Activation as a Therapeutic Target for Olfactory Dysfunction in Chronic Rhinosinusitis

Jinxiong Yang[1], Dong Wang[1,2], Shihan Liu[1], Renjing Luo[3], Wenlong Luo[1,*]

[1]Department of Otolaryngology-Head and Neck Surgery, The Second Affiliated Hospital of Chongqing Medical University, 400010 Chongqing, China
[2]Department of Otolaryngology-Head and Neck Surgery, Dazhou Central Hospital, 635000 Dazhou, Sichuan, China
[3]Department of Otolaryngology, The People's Hospital of Chongqing Liang Jiang New Area, 401147 Chongqing, China
*Correspondence: luowenlong@hospital.cqmu.edu.cn (Wenlong Luo)
Submitted: 10 July 2025 Revised: 18 August 2025 Accepted: 25 August 2025 Published: 20 September 2025

Background: Olfactory dysfunction (OD) is commonly associated with chronic rhinosinusitis (CRS), with T-helper 2 (Th2) cell polarization implicated in its pathogenesis. This study aimed to elucidate the role and underlying mechanism of the Th2-derived cytokine interleukin (IL)-4, acting via the phosphoinositide 3-kinase (PI3K)/Akt signaling pathway, in mediating olfactory epithelial injury during CRS-related OD.

Methods: The mechanism of Th2 cell dominance in CRS-associated OD through the IL-4/PI3K signaling pathway was investigated. A CRS model was established in age-matched senescence accelerated mouse resistant 1 (SAMR1) mice, with sneezing and scratching frequencies recorded. Flow cytometry quantified Th cell proportions and apoptosis, while quantitative reverse transcription polymerase chain reaction (RT-qPCR) and Western blotting (WB) assessed IL-4/interleukin-4 receptor (IL-4R), *IL-4*/*PI3K* pathway components, inflammatory/apoptotic markers, and olfactory-associated proteins. Following transfection of *IL-4R* short hairpin RNA (shRNA) into olfactory epithelial cells (efficiency confirmed by RT-qPCR and WB), a Th2 cell-olfactory epithelial cell co-culture system was established.

Results: CRS mice exhibited decreased olfactory marker protein (OMP) expression, upregulated phosphorylated- nuclearfactor-kappaB p65 (p-p65), enhanced IL-4/PI3K pathway activity, and elevated inflammatory/apoptotic markers. Th2 co-culture reduced olfactory epithelial cell viability, increased apoptosis, activated IL-4/PI3K signaling and inflammatory/apoptotic responses, and suppressed OMP expression. Notably, *IL-4R* knockdown reversed these alterations.

Conclusions: CRS modeling and Th2 co-culture reduces OMP expression, activates the p-p65/IL-4/PI3K pathway, and exacerbates inflammation and apoptosis, whereas *IL-4R* knockdown effectively counteracts these alterations.

Keywords: olfactory dysfunction; chronic rhinosinusitis; T-helper 2 polarization; IL-4; PI3K

Introduction

Olfactory dysfunction (OD) refers to a decreased or absent sense of smell [1]. Based on the pathological site and factors, OD is classified into paranasal sinus and non-sinonasal types [2,3], with the latter primarily associated with central nervous system conduction abnormalities [4]. This central OD is often associated with neurological disorders such as Parkinson's disease, Alzheimer's disease, and craniocerebral trauma [5,6]. In addition, OD arising primarily from dysfunction of olfactory epithelial cells, especially those influenced by chronic sinusitis and age-related degenerative diseases, has not received enough attention, and patients frequently delay medical consultation until olfactory function is markedly impaired or lost [7].

Chronic rhinosinusitis (CRS), especially CRS with nasal polyps (CRSwNP), frequently contributes to olfactory bulb dysfunction, which subsequently impairs olfactory epithelial function [8,9]. Previous studies have shown that CRSwNP represents a typical inflammatory disease mediated by type 2 T-helper (Th2) cells, characterized by increased eosinophilia and enhanced Th2 cytokine production [10,11]. Th2 cells and their cytokines interact to initiate a cascade response, promote eosinophil recruitment, and drive the onset and progression of inflammation [12,13]. Moreover, Th2 cytokines, including *IL-4*, *IL-5*, and *IL-13*, mediate epithelial fibrosis and mucus metaplasia, accelerate eosinophil infiltration, and participate in tissue remodeling [14,15].

Activation of the PI3K/Akt signaling axis has been shown to induce the differentiation of T-helper cells into the Th2 phenotype, leading to the secretion of cytokines such as IL-4, IL-5, and tumor necrosis factor alpha (TNF-α), and other inflammatory factors [16,17]. Furthermore, the PI3K/Akt axis stimulates B helper cells to produce immunoglobulin E (IgE), thereby mediating type I allergic re-

actions through eosinophil differentiation, aggregation, activation, and degranulation [18,19]. Conversely, the specific PI3K inhibitor LY294002 markedly downregulates the phosphorylation of Akt in murine lung tissue, inhibiting the secretion of Th2 cytokines, the infiltration of eosinophils, and the production of mucus [20,21].

In this study, the role of the key cytokine IL-4 within the Th2 inflammatory microenvironment was investigated, with a focus on its effects on olfactory epithelial cells in CRS and underlying mechanisms. These findings provide new evidence to support CRS diagnosis and treatment strategies targeting the Th2 immune response.

Materials and Methods

Establishment of the CRS Mouse Model

A total of 12 male specific-pathogen-free (SPF) SAMR1 mice (n = 12, 3–6 months old, body weight = 30 ± 0.9 g) were obtained from Huachuang Sino (Taizhou, China). Mice were randomly divided into a control group (Control group) and a chronic rhinosinusitis group (CRS group), with six mice in each group. Model induction began after one week of adaptive feeding. On days 0, 7, and 14 of the experiment, mice received intraperitoneal injections of 100 µL of ovalbumin (OVA, 1 mg/mL) for sensitization, while controls received equal volumes of saline. Beginning on day 21, 10 µL OVA nasal drops (100 mg/mL) were administered into both nostrils once daily for seven consecutive days. Controls received saline in the same manner. Starting from day 28, nasal drops were administered three times per week. After instilling 10 µL of OVA solution into each nostril for 15 min, 10 µL staphylococcal enterotoxin B (SEB) bacterial solution was administered, while controls received saline solution accordingly.

All animal experiments complied with the ARRIVE guidelines and were conducted in accordance with the National Institutes of Health Guide for the Care and Use of Laboratory Animals (NIH Publication No. 8023, revised 1978). Experimental protocols were approved by the Institutional Animal Care and Use Committee of the Second Affiliated Hospital of Chongqing Medical University (approval number: IACUC-SAHCQMU-2023-0069). Mice were euthanized by CO_2 asphyxiation.

Olfactory Dysfunction (OD) Test

Before testing, animals were acclimated to the test box for 30 min daily over three consecutive days. Food was withheld for 12 hours before the experiment. During testing, a 3-cm bedding layer was placed in the test container, and a 0.5 g food pellet was randomly buried 0.5 cm beneath the surface. Each mouse was placed in the box, and timing started immediately. The search time ended when the mouse uncovered and grasped the food pellet with its forepaws or teeth, and the duration of the search was recorded.

Flow Cytometric Analysis

Cells (3×10^5/well) were seeded and cultured in 6-well plates. Apoptotic cells were stained using an Annexin V/PI Apoptosis Detection Kit (C1062M, Beyotime, Shanghai, China) according to the manufacturer's instructions and analyzed with a FACSCalibur flow cytometer (BD, Becton Dickinson, Franklin Lakes, NJ, USA).

Hematoxylin and Eosin (H&E) Staining

Olfactory epithelial tissues were fixed in 10% formaldehyde (BL539A, Biosharp, Hefei, China) for 24 h, washed in 10% EDTA (798641, Sigma, St. Louis, MO, USA) decalcification solution, embedded in paraffin, and sectioned into 4-µm thickness using a Leica RM2235 microtome (Leica Biosystems, Wetzlar, Germany). Sections were stained with hematoxylin for 3 min and eosin for 1 min, dehydrated, and mounted with neutral resin (C0105S, Beyotime, Shanghai, China). Images were captured using an OLYMPUS IX71 microscope (IX71, Tokyo, Japan) at 200× magnification, with scale bars indicated.

Immunohistochemistry (IHC)

Olfactory epithelial tissue sections were deparaffinized, rehydrated, and subjected to antigen retrieval with repair solution (C1032, Solarbio, Beijing, China) at 98 °C for 20 min, followed by incubation in 3% H_2O_2 (SI125-01, SEVENBIO, Beijing, China) at room temperature (RT) for 20 min. After PBS (P1020, Solarbio, Beijing, China) washing, sections were treated with 0.1% Triton X-100 for 10 min and incubated overnight at 4 °C with diluted antibodies: olfactory marker protein (1:200, DF13678, INTERLAB, Beijing, China) and phospho-NF-κB p65 (Ser468 1:200, 82335-1-RR, Proteintech, Rosemont, IL, USA). Sections were subsequently incubated with goat anti-rabbit IgG-HRP (1:200, PV9000, zsbio, Beijing, China) for 1 h at 37 °C in the dark. DAB solution (KGP1045-20, keyGEN, Nanjing, China) was applied for 15 min, and nuclei were counterstained with hematoxylin for 10 min. Images were captured with an Olympus IX71 microscope (OLYMPUSIX71, Tokyo, Japan).

Western Blotting

Total protein was extracted using a Total protein extraction kit for animal tissues/cells (BC3790 Solarbio Science & Technology Co., Ltd., Beijing, China), and concentrations were determined by a BCA assay (Biosharp, Hefei, China). Forty micrograms of protein per sample were separated by SDS-PAGE and transferred onto membranes, which were blocked with 5% BSA for 1.5 hours. Membranes were then incubated overnight at 4 °C with the following primary antibodies: anti-IL-4 (1:1000, 66142-1-Ig, Proteintech, Rosemont, IL, USA), anti-IL-13 (1:1000, DF6813, Affinity, San Diego, CA, USA), anti-IL-4R (1:1000, 28331-1-AP, Proteintech, Rosemont,

IL, USA), Anti-Insulin Receptor Substrate 1 (anti-IRS-1) (1:1000, 17509-1-AP, Proteintech, Rosemont, IL, USA), anti-PI3K (1:1000, bs-0128R, BIOSS, Beijing, China), Anti-phosphatidylinositol 3-kinase (anti-p-PI3K) (1:1000, bs-3332R, BIOSS, Beijing, China), anti-AKT (1:1000, bs-0115R, BIOSS, Beijing, China), anti-p-AKT (1:1000, bs-0876R, BIOSS, Beijing, China), anti-olfactory marker protein (anti-OMP) (1:1000, DF13678, Affinity, San Diego, CA, USA),anti-BCL2-associated X protein (anti-Bax) (1:1000, 12789-1-AP, Affinity, San Diego, CA, USA), anti-B-cell lymphoma-2 (anti-Bcl-2) (1:1000, 50599-2-Ig, Affinity, San Diego, CA, USA), anti-pro-cysteine-dependent aspartate-specific protease-3 (anti-pro-caspase-3) (1:1000, ab32499, Abcam, UK), anti-cleaved-caspase-3 (1:1000, ab214430, Abcam, UK), anti-p65 (1:1000, 10745-1-AP,Proteintech, Rosemont, IL, USA), anti-p-p65 (1:1000, 82335-1-RR, Proteintech, Rosemont, IL, USA), anti-IL-1β (1:1000, A16288, Abclonal, Wuhan, China), anti-TNF-α (1:1000, A24214, Abclonal, Wuhan, China), anti-transforming growth factor-β (anti-TGF-β) (1:1000, 21898-1-AP, Proteintech, Rosemont, IL, USA), anti-β-actin (1:3000, AC038, Abclonal, Wuhan, China).

After washing, membranes were incubated with goat anti-rabbit IgG-HRP (1:5000, AS014, Abclonal, Wuhan, China) or goat anti-mouse IgG-HRP (1:5000, AS003, Abclonal, Wuhan, China) for 2 h at RT. Protein bands were visualized using ECL reagent (#34580, Thermo Fisher, Waltham, USA) and imaged using a Tanon Chemi Dog 5200T system (Tanon, China). Band intensities were quantified using ImageJ software (NIH, Bethesda, MD, USA).

RT-qPCR

Total RNA was isolated using a Total RNA extraction kit (r1200, Solarbio Science & Technology Co., Ltd., Beijing, China) and reverse-transcribed into cDNA using a reverse transcription kit (KR116, Vazyme, Nanjing, China). Quantitative PCR was performed on a 7900 PCR system (Applied Biosystems) using SYBR Green Premix (1725122, Bio-Rad, Hercules, CA, USA). Relative mRNA levels were determined with the $2^{-\Delta\Delta Cq}$ method, normalized to β-actin. The primer sequences were:

IL-4R-F: 5′-ACGTGGTACAACCACTTCCA-3′;
IL-4R-R: 5′-TGCGGGTACTTGGTTGACTC-3′.
IRS-1-F: 5′-CAGCCTCTTCTTCTGCTTCTGTT-3′;
IRS-1-R: 5′-CCTTGAGTGTCTGCGCGAAT-3′.
PI3k-F: 5′-CGAGAGTGTCGTCACAGTGTC-3′;
PI3k-R: 5′-TGTTCGCTTCCACAAACACAG-3′.
Akt-F: 5′-ATGAACGACGTAGCCATTGTG-3′;
Akt-R: 5′-TTGTAGCCAATAAAGGTGCCAT-3′.
β-actin-F: 5′-GTCCCTCACCCTCCCAAAAG-3′;
β-actin-R: 5′-GCTGCCTCAACACCTCAACCC-3′.

Cell Culture and Treatment

Mouse olfactory epithelial (MOE) cells (CP-M149, Pricella, Wuhan, China) were cultured under standard conditions in DMEM medium supplemented with 10% FBS and 1% penicillin-streptomycin. MOE cells displayed a typical cobblestone-like appearance with tightly packed polygonal morphology, distinct borders, and centrally located nuclei, consistent with epithelial cell characteristics. Th2 cells (YS2817, Yaji Biology, Shanghai, China) were tested with a mycoplasma rapid detection kit (13100-01, SouthernBiotech, Birmingham, AL, USA) and verified to be mycoplasma-free. Both cell lines were authenticated by short tandem repeat (STR) profiling.

Screening of IL-4R shRNA

Cells were seeded in 6-well plates for culture. Before transfection, OPTI-MEM medium (12492013, Gibco, Carlsbad, CA, USA) was preheated in a water bath, and both the transfection reagent and DNA plasmid were equilibrated to room temperature. After adding 500 µL OPTI-MEM, LIPO2000 or 15 µg DNA was added, and the mixture was incubated at ambient temperature for 15 min. Following a 10-min standing period for DNA-liposome complex formation, the target cells were removed from the 37 °C incubator, gently washed twice with OPTI-MEM, and supplemented with 3 mL OPTI-MEM. After 15 min, 1 mL of the DNA-liposome mixture was added dropwise to the culture dish, mixed thoroughly, and incubated at 37 °C with 5% CO_2. Gene silencing was assessed by qRT-PCR. The target sequences of IL-4R shRNA and control (sh-NC) were as follows:

sh-IL-4R-1: GCCAGGAGTCAACCAAGTA;
sh-IL-4R-2: GCCCTTCCAGAATCCTGTT;
sh-IL-4R-3: CCAAGACACCCTCAAACTT;
sh-NC: TTCTCCGAACGTGTCACGT.

Statistical Analysis

Data were analyzed using GraphPad Prism version 8.0 (GraphPad Software LLC, San Diego, CA, USA) and are presented as the mean ± standard error of the mean (SEM). One-way analysis of variance (ANOVA) was performed to assess statistical differences between groups. A p-value < 0.05 was considered statistically significant.

Results

Construction of the CRS Mouse Model and Detection of OD

To confirm CRS model establishment, mice were evaluated 10 min after nasal drop administration at weeks 5, 7, and 11. Sneezing and scratching frequencies per minute were recorded, and averages were calculated. Compared to the controls, the CRS group exhibited markedly increased sneezing/scratching behavior (Fig. 1A) ($p < 0.05$). Furthermore, olfactory dysfunction testing revealed that foraging times were longer in model mice, averaging 60 s, compared to 20 s in controls (Fig. 1B) ($p < 0.05$). Flow cytometry analysis of single-cell suspensions demonstrated altered T-

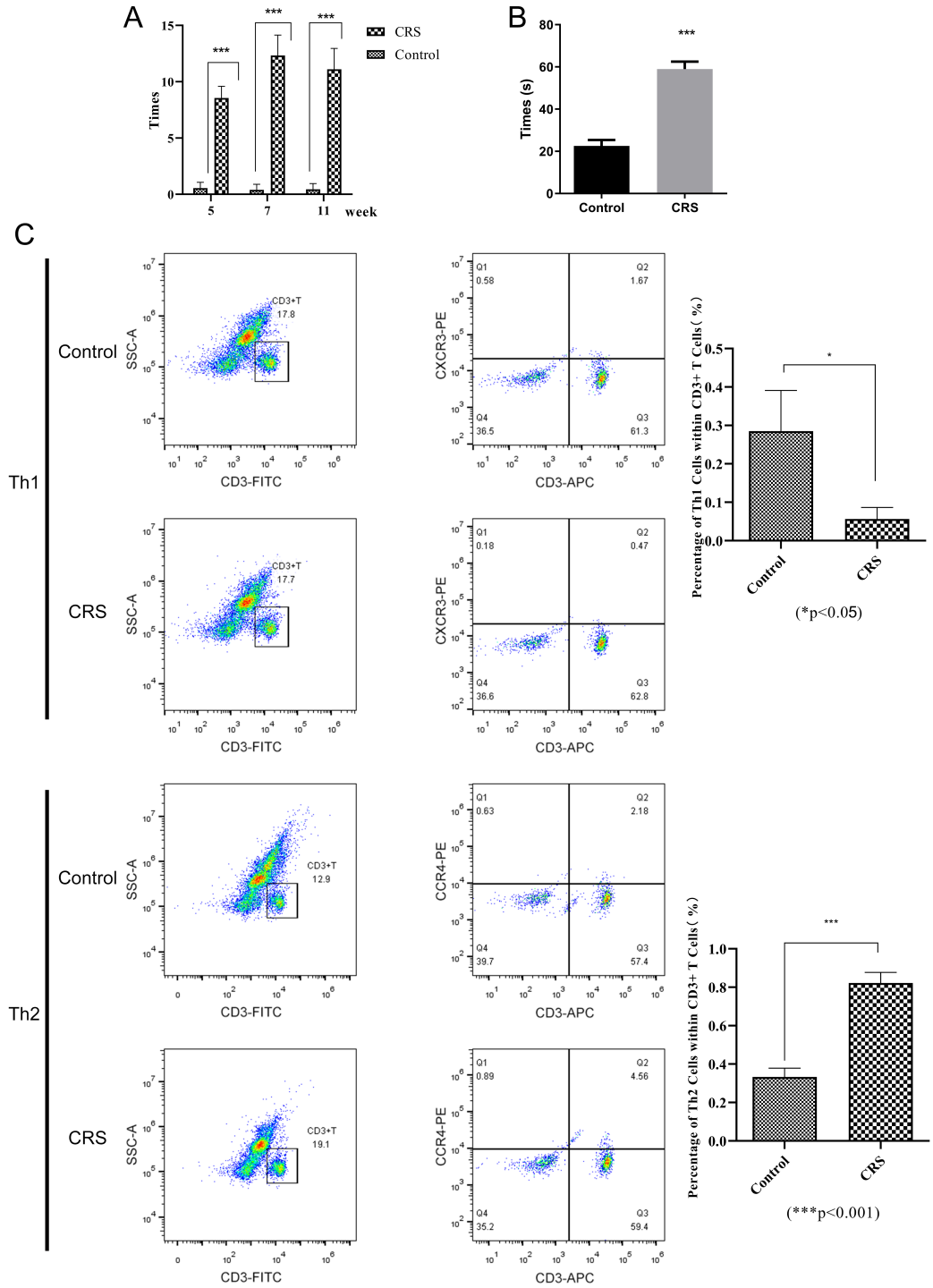

Fig. 1. Establishment of the CRS mouse model and detection of olfactory dysfunction. (A) Frequency of sneezing and nose scratching episodes per minute in mice. (B) Evaluation of the olfactory function using the olfactory foraging test. (C) Flow cytometry analysis of Th cells in single-cell suspensions of fresh nasal tissue samples. Data are presented as mean ± standard deviation. Statistical significance relative to the control group: $*p < 0.05$, $***p < 0.001$. CRS, chronic rhinosinusitis.

helper subsets. Relative to controls, the CRS group showed a reduced proportion of Th1 cells ($p < 0.05$) and an increased proportion of Th2 cells (Fig. 1C) ($p < 0.05$).

OMP Expression Is Reduced, and p-p65 Expression Is Increased in CRS Mice

First, H&E staining histological evaluation of mouse nasal tissue samples was performed to assess the pathological changes of CRS mice. The results demonstrated that

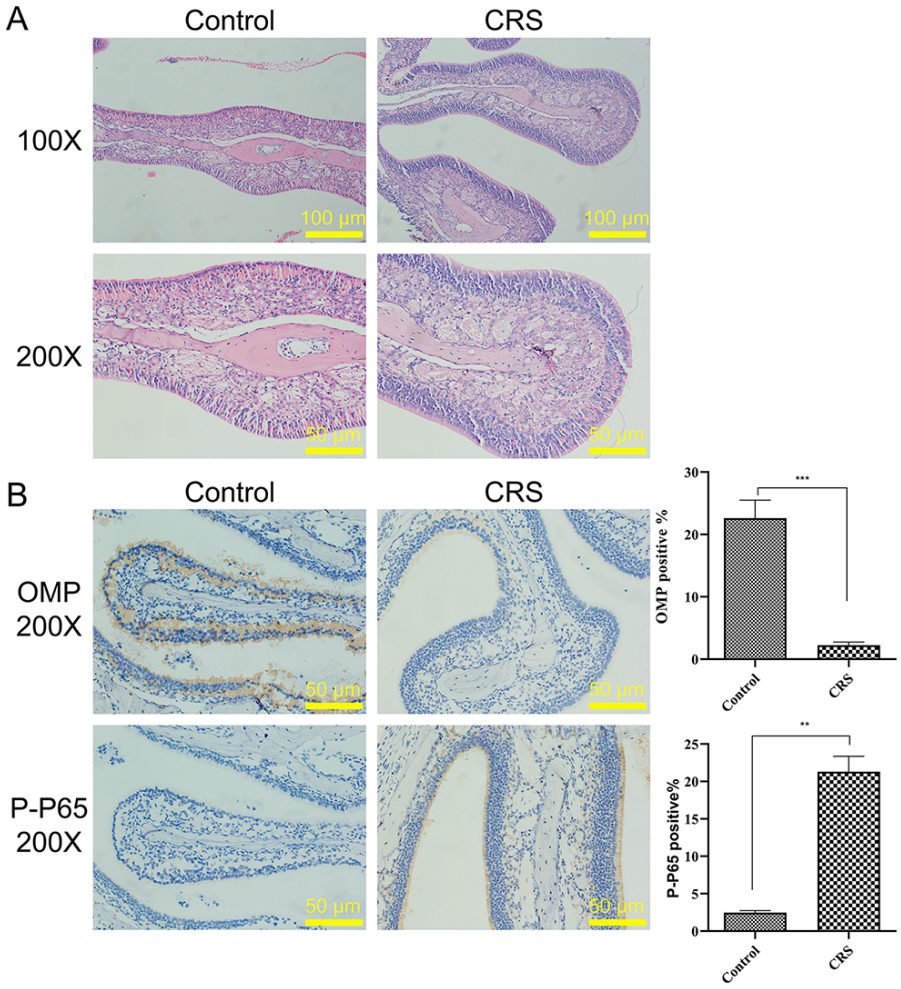

Fig. 2. Expression of OMP and phosphorylated p65 in CRS mice. (A) Representative H&E staining of nasal mucosa. (B) Immunohistochemical analysis of OMP and phosphorylated p65 expression in nasal tissues. Data are presented as mean ± standard deviation. Statistical significance relative to the control group: $^{**}p < 0.01$, $^{***}p < 0.001$. OMP, olfactory marker protein.

in the control group, the cilia of the olfactory epithelium were neatly aligned and upright, the basement membrane thickness was uniform with a clear boundary to the matrix, no significant inflammatory cell infiltration was observed, and the glands exhibited neither hyperplasia nor dilation. In contrast, the CRS group exhibited epithelial damage, ciliary destruction and thickening, irregular basement membrane thickness with blurred boundaries to the matrix, inflammatory cell infiltration, and mild irregular glandular hyperplasia (Fig. 2A).

Immunohistochemistry was performed to evaluate the expression of the olfactory marker OMP and p-p65 in tissue samples. In the control group, cytoplasmic staining was brown with abundant OMP-positive signals ($p < 0.05$), whereas in the CRS group, the p-p65-positive signal was significantly enhanced ($p < 0.05$). These findings indicated that, compared with the control group, OMP expression was decreased while p-p65 expression was increased in the CRS group (Fig. 2B).

Levels of IL-4/IL-4R, PI3K/Akt Axis Components, Inflammatory Factors, Apoptotic Factors, and Olfactory-Related Marker Proteins in CRS Mice

To investigate the expression of *IL-4*/*IL-4R*, *PI3K*/*Akt* signaling pathway components, inflammatory mediators, apoptosis-related proteins, and olfactory-associated markers in CRS mice, RT-qPCR and Western blotting were conducted. The RT-qPCR results demonstrated that *IL-4R*, *IRS-1*, *PI3K*, and *Akt* axis transcripts were significantly upregulated in the CRS group compared to the control group (Fig. 3) ($p < 0.05$). Western blotting further demonstrated elevated protein levels of IL-4, IL-13, IL-4R, IRS-1, p-PI3K, p-Akt, the NF-κB activation marker p-p65, and the inflammatory cytokines IL-1β, TNF-α, and TGF-β in the CRS group compared to the controls. Additionally, apoptosis-related proteins were altered, with increased Bax and cleaved caspase-3, along with reduced Bcl-2. Furthermore, the levels of the olfactory marker protein OMP were reduced. These alterations were consistent with enhanced

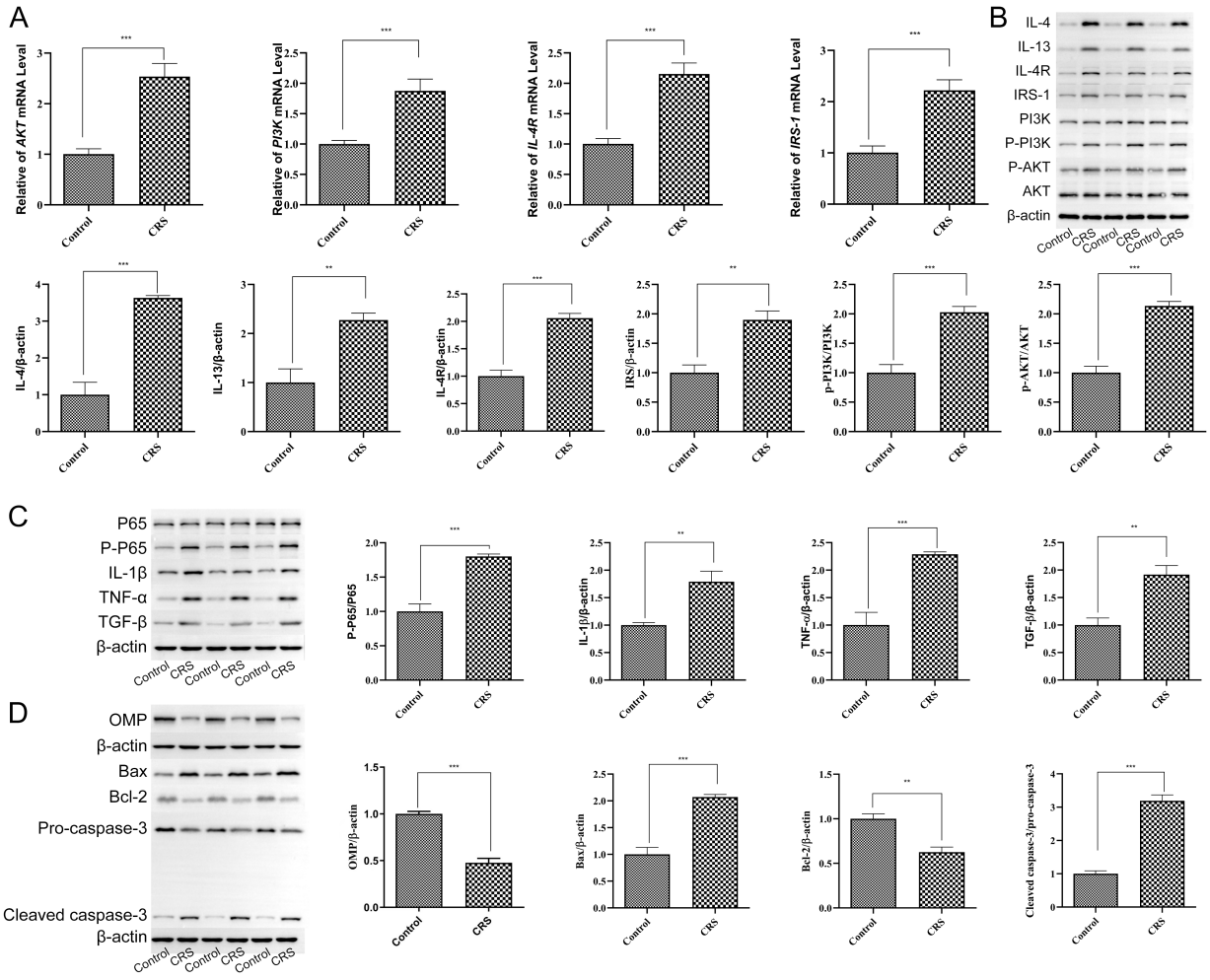

Fig. 3. Expression of IL-4/IL-4R, PI3K/Akt components, inflammatory factors, apoptotic markers, and olfactory-related marker proteins in CRS mice. (A) RT-qPCR analysis of IL-4/PI3K/Akt axis-related factors in olfactory epithelial tissues of control and CRS mice. (B–D) Western blot analysis of IL-4/IL-4R and PI3K/Akt pathway components, inflammatory factors, apoptotic factors, and olfactory-related markers in olfactory epithelial tissue. Data are presented as mean ± standard deviation. Statistical significance relative to the control group: $^{**}p < 0.01$, $^{***}p < 0.001$. RT-qPCR, quantitative reverse transcription polymerase chain reaction.

phosphorylation of PI3K and Akt, indicating activation of the PI3K/Akt signaling pathway in the CRS group compared to the control group ($p < 0.05$).

Construction of a Co-Culture System of Th2 Cells and Olfactory Epithelial Cells and Its Effects on Cell Viability and Apoptosis

IL-4R shRNA was transfected into olfactory epithelial cells, and knockdown efficiency was verified by RT-qPCR. The sequence vector with the highest silencing efficiency was selected for subsequent experiments. Cell proliferation in olfactory epithelial cells was assessed by CCK-8 assays, and a co-culture system of T lymphocytes and olfactory epithelial cells was established. Experimental groups included: (1) olfactory epithelial cells alone; (2) co-culture of Th2 cells with olfactory epithelial cells; (3) *IL-4R* knockdown in olfactory epithelial cells; (4) *IL-4R* knockdown in olfactory epithelial cells with Th2 co-culture; (5) Olfactory epithelial cells transfected with KD-NC; and (6) KD-NC-transfected olfactory epithelial cells with Th2 co-culture.

Comparisons revealed that groups 1 vs. 2 and 5 vs. 6 showed reduced cell viability when olfactory epithelial cells were co-cultured with Th2 cells relative to cell cultures alone. Furthermore, group 4 vs. 6 demonstrated that IL-4R knockdown in olfactory epithelial cells, combined with Th2 co-culture, significantly increased cell viability (Fig. 4A–C) ($p < 0.05$).

Effects of Th2 Cells and Olfactory Epithelial Cells Co-Culture System on the Expression of IL-4R/PI3K Signaling, Apoptosis, and Olfactory-Related Markers

RT-qPCR and Western blotting were utilized to evaluate the expression of *IL-4*/*PI3K* signaling components, apoptosis-associated factors, and olfactory-related marker factors in olfactory epithelial cells. The results indicated that the mRNA levels of *IL-4R*, and *IRS-1* were signifi-

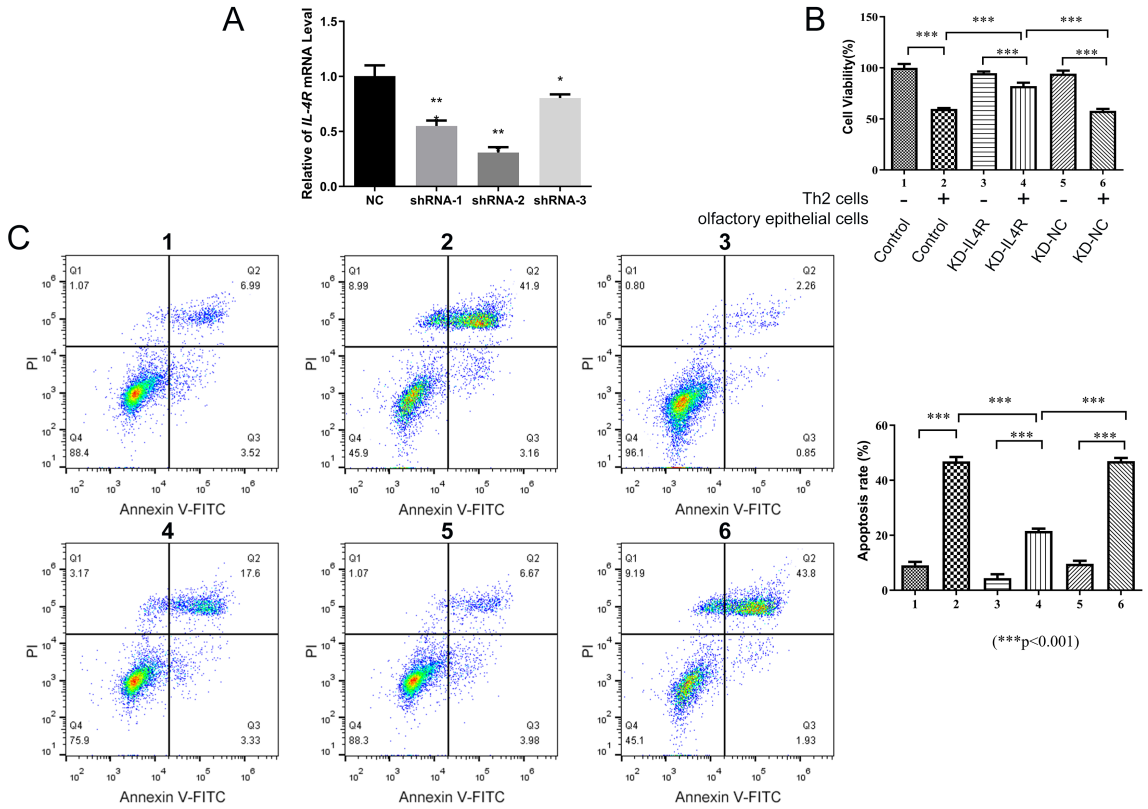

Fig. 4. Establishment of a Th2 cell-olfactory epithelial cell co-culture system and its effects on cell viability and apoptosis. (A) Construction of IL-4R shRNA vector for olfactory epithelial cell transfection, with transfection efficiency assessed by RT-qPCR. (B) CCK-8 to evaluate cell proliferation activity. (C) Flow cytometry analysis of apoptosis. Data are presented as mean ± standard deviation. Statistical significance relative to the control group: $*p < 0.05$; $**p < 0.01$; $***p < 0.001$.

cantly upregulated in olfactory epithelial cells co-cultured with Th2, as determined by RT-qPCR (Fig. 5A) ($p < 0.05$). Western blot analysis further confirmed increased protein levels of p-PI3K and p-Akt, suggesting activation of the PI3K signaling pathway. Additionally, expression p-p65 was elevated. In terms of apoptosis, protein levels of Bax, and cleaved caspase-3 were upregulated, while Bcl-2 was downregulated. The olfactory marker protein OMP was also downregulated, as evidenced by both RT-qPCR and Western blot analysis (Fig. 5B) ($p < 0.05$). Mechanistically, Th2 cells secrete IL-4 ligands that bind to IL-4Rα on the olfactory epithelial cells, thereby recruiting the γc chain to form a functional receptor complex. Notably, knockdown of *IL-4R* expression in olfactory epithelial cells reversed the co-culture-induced upregulation of *IL-4*/*PI3K* signaling pathway components, inflammatory and apoptotic factors, as well as the downregulation of OMP.

Discussion

The development of CRS is associated with both extrinsic and intrinsic factors, such as microbial infection or factors predisposing individuals to disproportionate inflammatory responses [22]. CRS is commonly classified into patients with CRSwNP and those without polyps (CRSsNP), with CRSwNP representing a chronic type 2 (T2)-biased inflammation of the sinonasal mucosa [23]. Th2 inflammation remains a key factor in the pathogenesis of CRSwNP [24]. In this study, we established a CRS mouse model and assessed the expression of *IL-4*/*IL-4R* and *PI3K*/*Akt* pathway components, along with inflammatory factors, apoptosis-associated factors, and olfactory-related markers. Subsequently, a co-culture system of Th2 cells and olfactory epithelial cells was constructed to investigate its effects on cell viability, apoptosis, and regulation of the *IL-4R*/*PI3K* axis, apoptosis, and olfactory-related markers.

Our findings indicated that sneezing and scratching frequencies were significantly higher in the CRS group compared to the control group. Foraging experiments further revealed that foraging duration was prolonged in CRS mice relative to the controls [25]. Flow cytometry analysis revealed that, compared with the control group, the proportion of Th1 cells was reduced in the CRS group, while the proportion of Th2 cells was increased. Histological analysis reveals epithelial damage in the nasal mucosa of CRS mice, characterized by ciliary destruction and thickening with poorly defined boundaries, infiltration of inflammatory cells, and irregular glandular hyperplasia, consis-

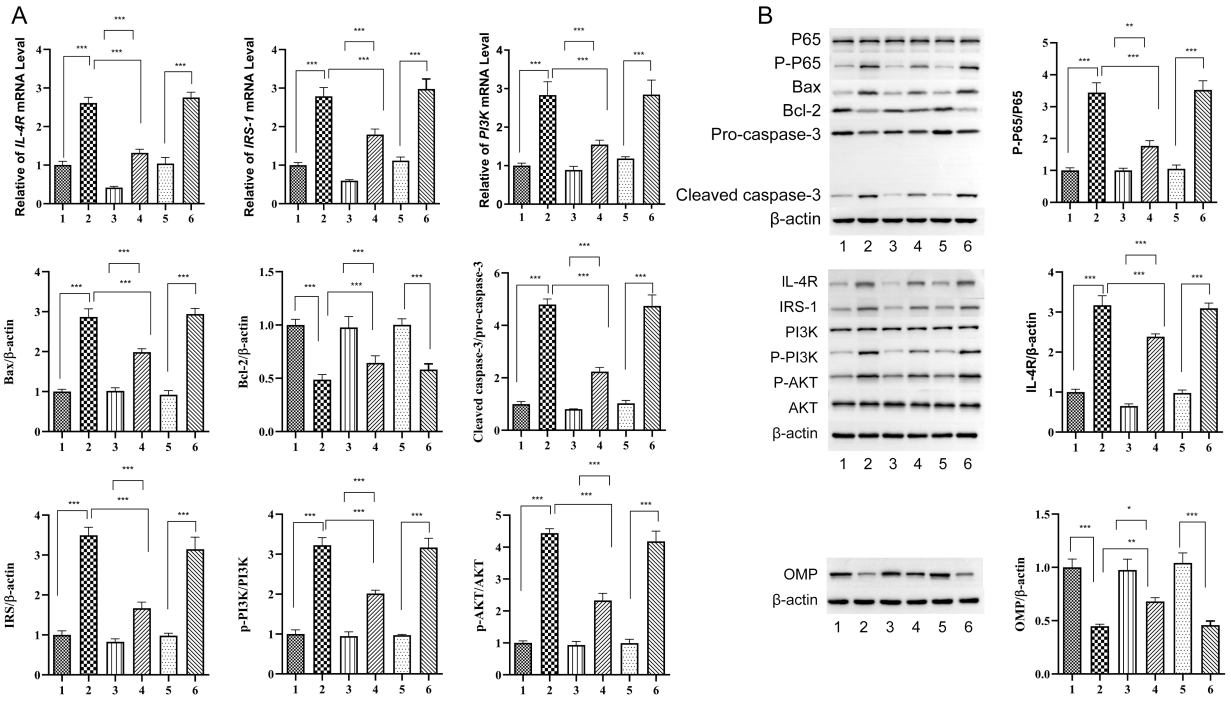

Fig. 5. Impact of Th2-olfactory epithelial cell co-culture on IL-4R/PI3K signaling, apoptosis, and olfactory-related markers. (A) RT-qPCR analysis of IL-4R/PI3K pathway components, apoptotic factors, and olfactory-related markers in olfactory epithelial cells. (B) Western blot evaluation of IL-4R/PI3K pathway components, apoptotic factors, and olfactory-related markers in olfactory epithelial cells. Data are presented as mean ± standard deviation. Statistical significance relative to the control group: $*p < 0.05$, $**p < 0.01$, $***p < 0.001$.

tent with previous reports [26]. Moreover, immunohistochemistry demonstrated reduced expression of the olfactory marker OMP, accompanied by elevated levels of p-p65 in CRS mice compared to controls.

CRS is frequently associated with eosinophilic inflammation and elevated levels of Th2 cytokines, typically IL-4 and IL-13 [27]. Similarly, our study revealed upregulation of IL-4/PI3K-associated components (IL-4, IL-13, IL-4R, IRS-1, p-PI3K, and p-Akt), and increased levels of inflammatory factors (p-p65, IL-1β, TNF-α, and TGF-β) in CRS mice. Moreover, the apoptotic regulators Bax, pro-caspase-3, and cleaved caspase-3 were upregulated, while Bcl-2 expression was reduced. The expression of olfactory marker proteins, including OMP, was also reduced.

In this study, after co-culture of Th2 cells and olfactory epithelial cells, the expression of IL-4/PI3K components (IL-4, IL-13, IL-4R, IRS-1, p-PI3K, p-Akt) and inflammatory mediators (p-p65, IL-1β, TNF-α, and TGF-β) was significantly upregulated. Moreover, the levels of the apoptotic factors Bax, pro-caspase-3, and cleaved caspase-3 were increased, while those of Bcl-2, olfactory marker protein, and receptor OMP were reduced. Notably, knockdown of *IL-4R* expression in olfactory epithelial cells reversed the expression of these molecules. Deletion of *IL-4R* not only blocks the IL-4 signaling but also induces sustained inhibition of downstream JAK1/STAT6, resulting in mitochondrial Reactive oxygen species(ROS) accumulation [28]. Elevated ROS promotes irreversible cell cycle arrest by activating p38-MAPK, and this effect remains difficult to reverse even with exogenous IL-4 [29]. Although co-culture with Th2 cells supplements IL-4, the deletion of IL-4R renders olfactory epithelial cells unresponsive to other Th2-derived pro-survival factors (such as IL-13, AREG), leading to no recovery in overall viability [30]. Therefore, knockdown of *IL-4R* expression in olfactory epithelial cells reversed the upregulation of *IL-4*/*PI3K* signaling, inflammatory and apoptotic mediators, and the downregulation of olfactory marker protein OMP observed after Th2 co-culture.

Collectively, OMP expression was reduced in CRS mice, while p-p65 expression, and IL-4/PI3K signaling pathway, inflammation- and apoptosis-related factors were upregulated. In the Th2-olfactory epithelial cell co-culture system, cell viability decreased, apoptosis increased, the IL-4/PI3K signaling and inflammatory/apoptotic factors were upregulated, whereas olfactory marker proteins and receptor OMP were downregulated. Knockdown of *IL-4R* expression in olfactory epithelial cells reversed these molecular alterations.

However, this study has several limitations. First, the research was primarily based on animal models, and the findings may not fully represent the pathological and physi-

ological processes of human CRS [31]. Second, the *in vitro* cell culture conditions used in the study may differ from the *in vivo* microenvironment, which could limit the generalizability of the experimental results. Moreover, although we demonstrated that *IL-4R* knockdown affects olfactory epithelial cells, the precise molecular mechanisms were not comprehensively explored and require further clarification in future studies. Finally, the study mainly focused on Th2-olfactory epithelial cell interactions. Other subtypes of immune cells that may be involved in the pathogenesis of CRS, such as Th1 and Th17 cells, have been associated with asthma, intestinal disease and bone immune disease in previous studies were not extensively examined, highlighting the need for a more comprehensive investigation in future research [32–34].

Conclusions

In conclusion, Th2 cell polarization contributes to olfactory dysfunction in chronic rhinosinusitis (CRS) through activation of the *IL-4*/*PI3K* signaling pathway. In CRS mice, reduced olfactory marker protein (OMP) expression, elevated p-p65 levels, upregulated *IL-4*/*PI3K* signaling, and increased inflammatory/apoptotic factors are associated with behavioral symptoms such as sneezing and scratching. Notably, the co-culture of Th2 cells with olfactory epithelial cells reproduces these pathological effects. Specifically, it suppresses cell viability, promotes apoptosis, activates the *IL-4*/*PI3K* pathway, and downregulates OMP expression. The reversal of these pathological changes following *IL-4R* knockdown in olfactory epithelial cells underscores *IL-4R* as a central mediator of Th2-induced damage. Collectively, these findings identify the *IL-4R*/*IL-4*/*PI3K* axis as a key mechanism in CRS-related olfactory impairment and highlight *IL-4R* blockade as a potential therapeutic strategy.

Availability of Data and Materials

The datasets used and/or analyzed during the current study are available from the corresponding author on reasonable request.

Author Contributions

JY and WL conceived and designed the experiments. JY and DW performed the experimental operation, data preservation, and literature search. RL and SL performed the data analysis and visualization. WL provided technical support and supervision. JY wrote the first draft of the manuscript, and WL revised it. All authors contributed to critical revision of the manuscript for important intellectual content. All authors read and approved the final manuscript. All authors have participated sufficiently in the work and agreed to be accountable for all aspects of the work.

Ethics Approval and Consent to Participate

All animal experiments were approved by the Institutional Animal Care and Use Committee of the Second Affiliated Hospital of Chongqing Medical University (approval number: IACUC-SAHCQMU-2023-0069) and followed the ARRIVE list.

Acknowledgment

Not applicable.

Funding

This research received no external funding.

Conflict of Interest

The authors declare no conflict of interest.

References

[1] Palmquist E, Larsson M, Olofsson JK, Seubert J, Bäckman L, Laukka EJ. A Prospective Study on Risk Factors for Olfactory Dysfunction in Aging. The Journals of Gerontology. Series A, Biological Sciences and Medical Sciences. 2020; 75: 603–610. https://doi.org/10.1093/gerona/glz265.

[2] Su B, Bleier B, Wei Y, Wu D. Clinical Implications of Psychophysical Olfactory Testing: Assessment, Diagnosis, and Treatment Outcome. Frontiers in Neuroscience. 2021; 15: 646956. https://doi.org/10.3389/fnins.2021.646956.

[3] Chan LP, Wang LF, Tai CF, Wu CC, Kuo WR. Huge sphenoid sinus olfactory neuroblastoma: a case report. The Kaohsiung Journal of Medical Sciences. 2009; 25: 87–92. https://doi.org/10.1016/S1607-551X(09)70046-4.

[4] Tremblay C, Mei J, Frasnelli J. Olfactory bulb surroundings can help to distinguish Parkinson's disease from non-parkinsonian olfactory dysfunction. NeuroImage. Clinical. 2020; 28: 102457. https://doi.org/10.1016/j.nicl.2020.102457.

[5] Dan X, Wechter N, Gray S, Mohanty JG, Croteau DL, Bohr VA. Olfactory dysfunction in aging and neurodegenerative diseases. Ageing Research Reviews. 2021; 70: 101416. https://doi.org/10.1016/j.arr.2021.101416.

[6] Frasnelli J, Laguë-Beauvais M, LeBlanc J, Alturki AY, Champoux MC, Couturier C, *et al*. Olfactory function in acute traumatic brain injury. Clinical Neurology and Neurosurgery. 2016; 140: 68–72. https://doi.org/10.1016/j.clineuro.2015.11.013.

[7] Borgmann-Winter KE, Rawson NE, Wang HY, Wang H, Macdonald ML, Ozdener MH, *et al*. Human olfactory epithelial cells generated in vitro express diverse neuronal characteristics. Neuroscience. 2009; 158: 642–653. https://doi.org/10.1016/j.neuroscience.2008.09.059.

[8] Kim JY, Ko I, Kim MS, Yu MS, Cho BJ, Kim DK. Association of Chronic Rhinosinusitis With Depression and Anxiety in a Nationwide Insurance Population. JAMA Otolaryngology– Head & Neck Surgery. 2019; 145: 313–319. https://doi.org/10.1001/jamaoto.2018.4103.

[9] Jiang L, Zeng Y, Huang Z, Tang Y, Zeng Q, Liu W, *et al*. Immunopathologic characteristics of Chinese pediatric patients with chronic rhinosinusitis. The World Allergy Organization Journal. 2021; 14: 100616. https://doi.org/10.1016/j.waojou.2021.100616.

[10] Lan F, Zhang N, Holtappels G, De Ruyck N, Krysko O, Van

Crombruggen K, *et al*. Staphylococcus aureus Induces a Mucosal Type 2 Immune Response via Epithelial Cell-derived Cytokines. American Journal of Respiratory and Critical Care Medicine. 2018; 198: 452–463. https://doi.org/10.1164/rccm.201710-2112OC.

[11] Schmidt H, Braubach P, Schilpp C, Lochbaum R, Neuland K, Thompson K, *et al*. IL-13 Impairs Tight Junctions in Airway Epithelia. International Journal of Molecular Sciences. 2019; 20: 3222. https://doi.org/10.3390/ijms20133222.

[12] Rocha VZ, Folco EJ, Sukhova G, Shimizu K, Gotsman I, Vernon AH, *et al*. Interferon-gamma, a Th1 cytokine, regulates fat inflammation: a role for adaptive immunity in obesity. Circulation Research. 2008; 103: 467–476. https://doi.org/10.1161/CIRCRESAHA.108.177105.

[13] Rahimi RA, Nepal K, Cetinbas M, Sadreyev RI, Luster AD. Distinct functions of tissue-resident and circulating memory Th2 cells in allergic airway disease. The Journal of Experimental Medicine. 2020; 217: e20190865. https://doi.org/10.1084/jem.20190865.

[14] Han M, Hu R, Ma J, Zhang B, Chen C, Li H, *et al*. Fas Signaling in Dendritic Cells Mediates Th2 Polarization in HDM-Induced Allergic Pulmonary Inflammation. Frontiers in Immunology. 2018; 9: 3045. https://doi.org/10.3389/fimmu.2018.03045.

[15] Liou CJ, Chen YL, Yu MC, Yeh KW, Shen SC, Huang WC. Sesamol Alleviates Airway Hyperresponsiveness and Oxidative Stress in Asthmatic Mice. Antioxidants (Basel, Switzerland). 2020; 9: 295. https://doi.org/10.3390/antiox9040295.

[16] Wu X, Gowda NM, Kawasawa YI, Gowda DC. A malaria protein factor induces IL-4 production by dendritic cells via PI3K-Akt-NF-κB signaling independent of MyD88/TRIF and promotes Th2 response. The Journal of Biological Chemistry. 2018; 293: 10425–10434. https://doi.org/10.1074/jbc.AC118.001720.

[17] Han Y, Yao R, Yang Z, Li S, Meng W, Zhang Y, *et al*. Interleukin-4 activates the PI3K/AKT signaling to promote apoptosis and inhibit the proliferation of granulosa cells. Experimental Cell Research. 2022; 412: 113002. https://doi.org/10.1016/j.yexcr.2021.113002.

[18] Li J, Zou C, Liu Y. Amelioration of Ovalbumin-Induced Food Allergy in Mice by Targeted Rectal and Colonic Delivery of Cyanidin-3-O-Glucoside. Foods (Basel, Switzerland). 2022; 11: 1542. https://doi.org/10.3390/foods11111542.

[19] Yuan A, Zeng J, Zhou H, Liu Q, Rao Z, Gao M, *et al*. Anti-type I allergic effects of Jing-Fang powder extracts via PI3K/Akt pathway in vitro and in vivo. Molecular Immunology. 2021; 135: 408–420. https://doi.org/10.1016/j.molimm.2021.01.015.

[20] Bing W, Pang X, Qu Q, Bai X, Yang W, Bi Y, *et al*. Simvastatin improves the homing of BMSCs via the PI3K/AKT/miR-9 pathway. Journal of Cellular and Molecular Medicine. 2016; 20: 949–961. https://doi.org/10.1111/jcmm.12795.

[21] Yuan J, Liu Y, Yu J, Dai M, Zhu Y, Bao Y, *et al*. Gene knockdown of CCR3 reduces eosinophilic inflammation and the Th2 immune response by inhibiting the PI3K/AKT pathway in allergic rhinitis mice. Scientific Reports. 2022; 12: 5411. https://doi.org/10.1038/s41598-022-09467-4.

[22] Wang X, Cutting GR. Chronic rhinosinusitis. Advances in Oto-rhino-laryngology. 2011; 70: 114–121. https://doi.org/10.1159/000322487.

[23] Schleimer RP. Immunopathogenesis of Chronic Rhinosinusitis and Nasal Polyposis. Annual Review of Pathology. 2017; 12: 331–357. https://doi.org/10.1146/annurev-pathol-052016-100401.

[24] Chikumoto A, Oishi K, Hamada K, Hirano T, Kakugawa T, Kanesada K, *et al*. Sequential Biotherapy Targeting IL-5 and IL-4/13 in Patients with Eosinophilic Asthma with Sinusitis and Otitis Media. Biomolecules. 2022; 12: 522. https://doi.org/10.3390/biom12040522.

[25] Fang S, Li X, Wei X, Zhang Y, Ma Z, Wei Y, *et al*. Beneficial effects of hydrogen gas inhalation on a murine model of allergic rhinitis. Experimental and Therapeutic Medicine. 2018; 16: 5178–5184. https://doi.org/10.3892/etm.2018.6880.

[26] Cheng J, Chen J, Zhao Y, Yang J, Xue K, Wang Z. MicroRNA-761 suppresses remodeling of nasal mucosa and epithelial-mesenchymal transition in mice with chronic rhinosinusitis through LCN2. Stem Cell Research & Therapy. 2020; 11: 151. https://doi.org/10.1186/s13287-020-01598-7.

[27] Joo YH, Cho HJ, Jeon YJ, Kim JH, Jung MH, Jeon SY, *et al*. Therapeutic Effects of Intranasal Tofacitinib on Chronic Rhinosinusitis with Nasal Polyps in Mice. The Laryngoscope. 2021; 131: E1400–E1407. https://doi.org/10.1002/lary.29129.

[28] Han JY, Lim DW, Kwon O, Lee YJ, Choi HY, Jung HJ, *et al*. Hybrid Cannabis sativa L. inflorescences exert an anti-inflammatory effect through the modulation of MAPK/NF-κB/NLRP3 inflammasome and JAK1/STAT6 pathway in HaCaT cells. Frontiers in Pharmacology. 2025; 16: 1617180. https://doi.org/10.3389/fphar.2025.1617180.

[29] Shabbir S, Muslim M, Muthu SA, Pissurlenkar RRS, Fatima S, Ali A, *et al*. The cocrystal of 3-((4-(3-isocyanobenzyl) piperazine-1-yl) methyl) benzonitrile with 5-hydroxy isophthalic acid prevents protofibril formation of serum albumin. Journal of Biomolecular Structure & Dynamics. 2022; 40: 538–548. https://doi.org/10.1080/07391102.2020.1815585.

[30] Li X, Keady J, Ward R. Neighbourhoods and dementia: An updated realist review of the qualitative literature to inform contemporary practice and policy understanding. Dementia (London, England). 2021; 20: 2957–2981. https://doi.org/10.1177/14713012211023649.

[31] Zhu H, Qu S, Gong M, Xiang Y, Gan S, Teng Y, *et al*. Mechanisms, diagnosis, and treatment of olfactory dysfunction in rhinosinusitis. European Journal of Medical Research. 2025; 30: 474. https://doi.org/10.1186/s40001-025-02740-y.

[32] Li M, Gan C, Zhang R, Wang J, Wang Y, Zhu W, *et al*. TRAF5 regulates intestinal mucosal Th1/Th17 cell immune responses via Runx1 in colitis mice. Immunology. 2023; 170: 495–509. https://doi.org/10.1111/imm.13685.

[33] Luo W, Hu J, Xu W, Dong J. Distinct spatial and temporal roles for Th1, Th2, and Th17 cells in asthma. Frontiers in Immunology. 2022; 13: 974066. https://doi.org/10.3389/fimmu.2022.974066.

[34] Wang X, Sun B, Wang Y, Gao P, Song J, Chang W, *et al*. Research progress of targeted therapy regulating Th17/Treg balance in bone immune diseases. Frontiers in Immunology. 2024; 15: 1333993. https://doi.org/10.3389/fimmu.2024.1333993.